UNIVERSITI PUTRA MALAYSIA

CHARACTERIZATION AND DIELECTRIC PROPERTIES OF PURE AND Er-SUBSTITUTED Bi4Ti3O12 AND Bi5CrTi3O15 AURIVILLIUS CERAMICS

WONG YICK JENG

ITMA 2018 1

CHARACTERIZATION AND DIELECTRIC PROPERTIES OF PURE AND Er-SUBSTITUTED $Bi_4Ti_3O_{12}$ AND $Bi_5CrTi_3O_{15}$ AURIVILLIUS CERAMICS

By

WONG YICK JENG

Thesis Submitted to the School of Graduate Studies, Universiti Putra Malaysia, in Fulfilment of the Requirements for the Degree of Doctor of Philosophy

January 2018

Abstract of thesis presented to the Senate of Universiti Putra Malaysia in fulfilment of the requirement for the degree of Doctor of Philosophy

CHARACTERIZATION AND DIELECTRIC PROPERTIES OF PURE AND Er-SUBSTITUTED $Bi_4Ti_3O_{12}$ AND $Bi_5CrTi_3O_{15}$ AURIVILLIUS CERAMICS

By

WONG YICK JENG

January 2018

Chair: Jumiah binti Hassan, PhD
Faculty: Institute of Advanced Technology

Aurivillius compounds, $(Bi_2O_2)^{2+}(Bi_{n-1}Ti_nO_{3n+1})^{2-}$, are structurally constructed by alternately stacking n perovskite units of $(Bi_{n-1}Ti_nO_{3n+1})^{2-}$ with two fluorite-like layers of $(Bi_2O_2)^{2+}$. Three-layered $Bi_4Ti_3O_{12}$ system in this kind of compounds is extensively studied. In most cases, the modification is done by doping various types of rare-earth ions at Bi-site to reduce high electrical conductivity for more effective ferroelectric dielectrics. Unlike the three-layered Aurivillius systems, attention to the four-layered Aurivillius systems isostructural with $Bi_5FeTi_3O_{15}$ is scarce, especially $Bi_5CrTi_3O_{15}$. Such a case involving the magnetic Cr^{3+} ions was only reported from the analysis of powder neutron diffraction data.

Preparation of the Aurivillius compounds is commonly done by conventional solid state reaction method. However, this economical method requires high-temperature solid state reaction to reach single phase. Here, high energy milling at room temperature for the mechanosynthesis of Aurivillius compounds with $Bi_4Ti_3O_{12}$, $Bi_{3.25}Er_{0.75}Ti_3O_{12}$, $Bi_5CrTi_3O_{15}$, and $Bi_{4.25}Er_{0.75}CrTi_3O_{15}$ compositions is employed. These mechanosynthesized samples subjected to a range of sintering temperatures (700 – 1000°C) are systematically compared with the conventionally processed samples in terms of X-ray Diffraction (XRD) analysis, Field Emission Scanning Electron Microscopy (FE-SEM) observation, dielectric, and density measurements.

All the comparative results obtained point to the effectiveness of the high energy milling over the conventional processing technique as a more efficient solid-phase formation method in synthesizing the studied samples. This is first demonstrated by room-temperature XRD studies. The sintering temperature at which these mechanosynthesized compounds show complete formation of the pure phase are comparatively lower than those of conventionally processed samples as a result of the mechanochemical reaction by high energy milling.

Consequently, FE-SEM observations of the mechanosynthesized samples reveal distinct grain morphologies contrary to the plate-like grain morphologies in the conventionally processed samples, in which the latter display grain growth with increasing sintering temperature controlled by anisotropic grain boundary. For the mechanosynthesized $Bi_4Ti_3O_{12}$, triple junction controlled grain growth is evident, while the grain growth of mechanosynthesized $Bi_{4.25}Er_{0.75}CrTi_3O_{15}$ is discovered for the first time being governed via multiple ordered coalescence of nanocrystals. Also, the mechanochemical effect triggers the improved sintered densities in the mechanosynthesized samples. For this reason, the mechanosynthesized samples exhibit much higher room-temperature dielectric constant values in the frequency range of 100 Hz – 10 MHz.

All samples prepared by both methods exhibit common feature in the variation of dielectric constant with respect to frequency, which follows directly from the relationship between densification and sintering temperature. Moreover, very similar intrinsic frequency dispersion of dielectric responses could be observed, with the physical basis for the interpretation is based on the empirical fitting model of relaxation functions: Cole-Cole, Cole-Davidson, and Havriliak-Negami.

Besides comparison of methods, the influence of Er^{3+} dopant on the parent structure of $Bi_4Ti_3O_{12}$ and $Bi_5CrTi_3O_{15}$ is also investigated. The marked contributions of this dopant are from the grain growth inhibition due to the grain boundary segregation of Er^{3+} and weak low-frequency dispersion of the dielectric constant in the doped samples. These experimental evidences reflect the suppression of oxygen vacancies, which is also manifested in one of the fitting parameters, the reduced direct current conductivity.

Abstrak tesis yang dikemukakan kepada Senat Universiti Putra Malaysia sebagai memenuhi keperluan untuk ijazah Doktor Falsafah

PENCIRIAN DAN SIFAT DIELEKTRIK SERAMIK AURIVILLIUS $Bi_4Ti_3O_{12}$ DAN $Bi_5CrTi_3O_{15}$ DALAM BENTUK TULEN DAN Er-TERTUKAR GANTI

Oleh

WONG YICK JENG

Januari 2018

Pengerusi: Jumiah binti Hassan, PhD
Fakulti: Institut Teknologi Maju

Penstrukturan sebatian Aurivillius, $(Bi_2O_2)^{2+}(Bi_{n-1}Ti_nO_{3n+1})^{2-}$, adalah secara susunan selang n unit perovskit $(Bi_{n-1}Ti_nO_{3n+1})^{2-}$ dengan dua lapisan bak fluorit $(Bi_2O_2)^{2+}$. Sistem $Bi_4Ti_3O_{12}$ berlapis tiga dalam sebatian jenis ini telah dikaji dengan meluas. Dalam kebanyakan kes, ia diubah suai menerusi pendopan dengan pelbagai ion nadir bumi di tapak-Bi untuk mengurangkan kekonduksian elektrik demi feroelektrik dielektrik yang lebih berkesan. Tidak serupa dengan sistem Aurivillius berlapis tiga, perhatian kepada sistem Aurivillius berlapis empat yang isostruktur dengan $Bi_5FeTi_3O_{15}$ adalah kurang, terutamanya $Bi_5CrTi_3O_{15}$. Kes seperti ini yang melibatkan ion magnet Cr^{3+} hanya dilaporkan dari analisis data pembelauan neutron serbuk.

Penyediaan sebatian Aurivillius biasanya dilakukan dengan menggunakan kaedah tindak balas keadaan pepejal konvensional. Namun begitu, kaedah berekonomi ini memerlukan tindak balas keadaan pepejal yang bersuhu tinggi untuk mencapai fasa tunggal. Di sini, kisaran bertenaga tinggi pada suhu bilik digunakan untuk sintesis mekanik sebatian Aurivillius dengan komposisi $Bi_4Ti_3O_{12}$, $Bi_{3.25}Er_{0.75}Ti_3O_{12}$, $Bi_5CrTi_3O_{15}$, dan $Bi_{4.25}Er_{0.75}CrTi_3O_{15}$. Perbandingan sistematik bagi sampel-sampel tersintesis secara mekanik ini yang disinter pada julat suhu di antara 700 – 1000°C dengan sampel-sampel terproses scara konventional adalah dari segi analisis belauan sinar-X (XRD), cerapan mikroskopi elektron pengimbasan pancaran medan (FE-SEM), pengukuran dielektrik, dan ketumpatan.

Kesemua keputusan perbandingan yang diperoleh menghala tuju kepada keberkesanan kisaran bertenaga tinggi sebagai kaedah pembentukan fasa pepejal yang lebih cekap daripada teknik pemprosesan konvensional dalam mensintesiskan sampel kajian. Demonstrasi pertama ini adalah dari kajian XRD pada suhu bilik. Suhu pensinteran di mana sampel-sampel tersintesis secara mekanik ini

menunjukkan pembentukan lengkap fasa tulen adalah lebih rendah berbanding dengan sampel-sampel terproses scara konvensional akibat tindak balas kimia mekanik menerusi kisaran bertenaga tinggi.

Oleh sebab itu, permerhatian FE-SEM bagi sampel-sampel tersintesis secara mekanik mendedahkan morfologi butiran berbeza yang berlawanan dengan morfologi bak plat pada sampel-sampel terproses scara konventional, di mana morfologi yang kedua memaparkan pertumbuhan butiran dengan peningkatan suhu pensinteran yang dikawal secara sempadan butiran anisotropi. Bagi sampel $Bi_4Ti_3O_{12}$ yang tersintesis secara mekanik, pertumbuhan butiran kawalan simpangan tiga adalah jelas, sedangkan pertumbuhan bijian $Bi_{4.25}Er_{0.75}CrTi_3O_{15}$ dikawal melalui koalesens tertib berganda hablur nano merupakan penemuan yang pertama kali. Juga, kesan kimia mekanik mencetuskan penumpatan tersinter yang lebih baik dalam sampel. Atas sebab ini, sampel-sampel tersintesis secara mekanik menunjukkan nilai pemalar dielektrik yang lebih tinggi pada suhu bilik dalam julat frekuensi 100 Hz – 10 MHz.

Kesemua sampel yang disediakan oleh kedua-dua kaedah menunjukkan sifat sepunya dalam perubahan pemalar dielektrik merujuk kepada frekuensi, yang mana ianya mengikut secara langsung dari perhubungan antara penumpatan dan suhu pensinteran. Tambahan pula, serakan frekuensi intrinsik sambutan dielektrik yang sangat serupa dapat diperhatikan, dengan asas fizikal untuk pentafsiran adalah berdasarkan model penyuaian empirik fungsi kesantaian: Cole-Cole, Cole-Davidson, dan Havriliak-Negami.

Selain daripada kaedah bandingan, pengaruh dopan Er^{3+} terhadap struktur induk $Bi_4Ti_3O_{12}$ dan $Bi_5CrTi_3O_{15}$ turut disiasat. Sumbangan ketara dopan tersebut adalah dari perencatan pertumbuhan butiran disebabkan oleh pengasingan sempadan butiran Er^{3+} dan serakan frekuensi rendah pemalar dielektrik yang lemah dalam sampel-sampel terdop. Bukti-bukti eksperimen ini mencerminkan penindasan kekosongan oksigen, dinyatakan dalam salah satu parameter penyuaian juga, iaitu kekonduksian arus terus terkurang.

ACKNOWLEDGEMENTS

I would first and foremost like to thank my supervisor, Associate Professor Dr. Jumiah Hassan, for her kind guidance, patience, and advice throughout my PhD candidature in bringing this research to fruition. Not to forget Associate Professor Dr. Chen Soo Kien and Dr. Ismayadi Ismail for their precious time being part of my supervisory committee. I owe my deepest gratitude to the late Associate Professor Dr. Mansor Hashim, who has been so supportive in contributing insightful discussion and inspiring me consistently since year 2009. His way of explaining things clearly and vividly will be in the memory.

It was a great time to be in the scientific community at laboratory 231 and I would like to individually thank each one of my immediate colleagues for creating such a great working environment: Alex See, Wong Swee Yin, Tan Foo Khoon, Leow Chun Yan, Dayang, Mutia, Rafidah, Lee Chian Heng, and Tasiu. Among them, I am personally indebted to Alex, whose invaluable suggestions during the planning and development of this research are highly credited; and Swee Yin, for her guidance on the experimental and characterization procedures. It is a pleasure to pay high regards to Madam Norhaslinda for the collection of XRD data, and Madam Sarinawani for the FE-SEM images. Their technical assistances are greatly appreciated.

Last but not least, I would like to dedicate this work to my family. It would not have been possible for this work to see the light of the day without their moral support, encouragement, and loving understanding.

This PhD research is supported under continuing sponsorship from the Ministry of Higher Education, Malaysia, through a Fundamental Research Grant Scheme no. 01-02-14-1599FR.

I certify that a Thesis Examination Committee has met on 10 January 2018 to conduct the final examination of Wong Yick Jeng on his thesis entitled "Characterization and Dielectric Properties of Pure and Er-Substituted $Bi_4Ti_3O_{12}$ and $Bi_5CrTi_3O_{15}$ Aurivillius Ceramics" in accordance with the Universities and University Colleges Act 1971 and the Constitution of the Universiti Putra Malaysia [P.U.(A) 106] 15 March 1998. The Committee recommends that the student be awarded the Doctor of Philosophy.

Members of the Thesis Examination Committee were as follows:

Zainal Abidin bin Talib, PhD
Professor
Faculty of Science
Universiti Putra Malaysia
(Chairman)

Abdul Halim bin Shaari, PhD
Professor
Faculty of Science
Universiti Putra Malaysia
(Internal Examiner)

Hishamuddin bin Zainuddin, PhD
Associate Professor
Faculty of Science
Universiti Putra Malaysia
(Internal Examiner)

Raouf Abdle Hamid El-Mallawany, PhD
Professor
Menofia University
Egypt
(External Examiner)

NOR AINI AB. SHUKOR, PhD
Professor and Deputy Dean
School of Graduate Studies
Universiti Putra Malaysia

Date: 28 March 2018

This thesis was submitted to the Senate of Universiti Putra Malaysia and has been accepted as fulfilment of the requirement for the degree of Doctor of Philosophy. The members of the Supervisory Committee were as follows:

Jumiah binti Hassan, PhD
Associate Professor
Faculty of Science
Universiti Putra Malaysia
(Chairman)

Chen Soo Kien, PhD
Associate Professor
Faculty of Science
Universiti Putra Malaysia
(Member)

Ismayadi bin Ismail, PhD
Research Officer
Institute of Advanced Technology
Universiti Putra Malaysia
(Member)

Mansor bin Hashim, PhD
Associate Professor
Institute of Advanced Technology
Universiti Putra Malaysia
(Member)

ROBIAH BINTI YUNUS, PhD
Professor and Dean
School of Graduate Studies
Universiti Putra Malaysia

Date:

Declaration by graduate student

I hereby confirm that:

- this thesis is my original work;
- quotations, illustrations and citations have been duly referenced;
- this thesis has not been submitted previously or concurrently for any other degree at any other institutions;
- intellectual property from the thesis and copyright of thesis are fully-owned by Universiti Putra Malaysia, as according to the Universiti Putra Malaysia (Research) Rules 2012;
- written permission must be obtained from supervisor and the office of Deputy Vice-Chancellor (Research and Innovation) before thesis is published (in the form of written, printed or in electronic form) including books, journals, modules, proceedings, popular writings, seminar papers, manuscripts, posters, reports, lecture notes, learning modules or any other materials as stated in the Universiti Putra Malaysia (Research) Rules 2012;
- there is no plagiarism or data falsification/fabrication in the thesis, and scholarly integrity is upheld as according to the Universiti Putra Malaysia (Graduate Studies) Rules 2003 (Revision 2012-2013) and the Universiti Putra Malaysia (Research) Rules 2012. The thesis has undergone plagiarism detection software.

Signature: _____ Date: _____

Name and Matric No.: _____Wong Yick Jeng GS38080_____

Declaration by Members of Supervisory Committee

This is to confirm that:

- the research conducted and the writing of this thesis was under our supervision;
- supervision responsibilities as stated in the Universiti Putra Malaysia (Graduate Studies) Rules 2003 (Revision 2012-2013) are adhered to.

Signature: _____
Name of Chairman of Supervisory Committee: Jumiah binti Hassan

Signature: _____
Name of Member of Supervisory Committee: Chen Soo Kien

Signature: _____
Name of Member of Supervisory Committee: Ismayadi bin Ismail

Signature: _____
Name of Member of Supervisory Committee: Mansor bin Hashim

TABLE OF CONTENTS

LIST OF TABLES

LIST OF FIGURES

LIST OF ABBREVIATIONS

PZT	Lead zirconium titanate
Fe-RAMs	Ferroelectric random access memories
DRAMs	Dynamic random access memories
FE-PE	Ferroelectric-paraelectric phase transition
SHS	Self-propagating high-temperature synthesis
FTIR	Fourier transform infrared spectroscopy
TGA	Thermogravimetric analysis
DTA	Differential thermal analysis
XRD	X-ray diffraction
XPS	X-ray photoelectron spectroscopy
SEM	Scanning electron microscopy
TEM	Transmission electron microscopy
EDS	Energy dispersive X-ray spectroscopy
EXAFS	Extended X-ray absorption fine structure
BPR	Ball-to-powder weight ratio
MCA	Mechanochemical activation
SSR	Solid-state reaction
Log	Logarithm
CPE	Constant phase element
ICSD	Inorganic crystal structure database
FWHM	Breath of the peak at half of maximum intensity
CC	Cole-Cole
CD	Cole-Davidson
HN	Havriliak-Negami
IBLC	Internal barrier layer capacitor
SBLC	Surface barrier layer capacitor
MUT	Material under test
ESRF	European synchrotron radiation facility
LFD	Low-frequency dispersion
BTO-CM	Heat-treated Bi_2O_3-TiO_2 after conventional milling
BTO:Er^{3+}-CM	Heat-treated Bi_2O_3-Er_2O_3-TiO_2 after conventional milling
BCTO-CM	Heat-treated Bi_2O_3-Cr_2O_3-TiO_2 after conventional milling
BCTO:Er^{3+}-CM	Heat-treated Bi_2O_3-Er_2O_3-Cr_2O_3-TiO_2 after conventional milling
BTO-HM	Heat-treated Bi_2O_3 -TiO_2 after high energy milling
BTO:Er^{3+}-HM	Heat-treated Bi_2O_3-Er_2O_3- TiO_2 after high energy milling
BCTO-HM	Heat-treated Bi_2O_3- Cr_2O_3-TiO_2 after high energy milling
BCTO:Er^{3+}-HM	Heat-treated Bi_2O_3-Er_2O_3-Cr_2O_3-TiO_2 after high energy milling

LIST OF SYMBOLS

n	Number of oxygen octahedra in the pseudo-perovskite blocks
a	Crystallographic a-axis
b	Crystallographic b-axis
c	Crystallographic c-axis
A	Cationic site occupied by a mono, di, or trivalent large cation
B	Cationic site occupied by a tri, penta, or hexavalent small cation
A'	Alkali metal cation of Dion-Jacobson phase
x+	Formal charge associated with A cation
y+	Formal charge associated with B cation
T_{Curie}	Curie temperature
$T_{melting}$	Melting temperature
T_{sinter}	Sintering temperature
T_{DTG}	Derivative peak temperature
ΔT_{relax}	Degree of relaxation behaviour
a_o, b_o, c_o	Orthorhombic lattice parameters
a_T, c_T	Tetragonal lattice parameters
a_m, b_m, c_m	Monoclinic lattice parameters
V_m	Monoclinic unit cell volume
V_o	Orthorhombic unit cell volume
δ	Orthorhombicity
ρ_{XRD}	Theoretical X-ray density
+q	Positive charge
−q	Negative charge
μ_d	Dipole moment
l	Finite distance
E	Electric field
D	Phase of induction
α_m	Molecular polarisability
x(t)	Time variable displacement
γ	Damping coefficient
W	Potential energy
$\Gamma_{i,j}$	Charge transfer rate
$r_{i,j}$	Hopping distance
ξ	Localization length
$\Delta_{i,j}$	Transition energy
f	Frequency in Hz
ω	Angular frequency in rad/s
ω_R	Resonant angular frequency
$\varepsilon'_{r(max)}$	Maximum for the real part of the complex relative permittivity

$\varepsilon''_{r(max)}$	Maximum for the imaginary part of the complex relative permittivity
ε_0	Permittivity of free space
ε_r^*	Complex relative permittivity
ε'_r	Real part of the complex relative permittivity or dielectric constant
ε''_r	Imaginary part of the complex relative permittivity or dielectric loss
$\varepsilon'_{r(\infty)}$	High-frequency limit of dielectric constant
$\varepsilon'_{r(s)}$	Static value of low-frequency dielectric constant
$\varepsilon''_{r\,(CC)}$	CC-derived dielectric loss
$\varepsilon''_{r\,(CD)}$	CD-derived dielectric loss
$\varepsilon''_{r\,(HN)}$	HN-derived dielectric loss
C^*	Complex capacitance
C'	Real part of the complex capacitance
C''	Imaginary part of the complex capacitance
C_0	Capacitance of empty cell
$\tan\delta$	Dissipation factor
i	Imaginary operator with $(-1)^{1/2}$
M^*	Complex dielectric modulus
M'	Real part of the complex dielectric modulus
M''	Imaginary part of the complex dielectric modulus
Z^*	Complex impedance
Z'	Real part of the complex impedance
Z''	Imaginary part of the complex impedance
G_p	Parallel conductance
C_p	Parallel capacitance
R_p	Parallel resistance
C_s	Series capacitance
R_s	Series resistance
R_{el}	Electrode resistance
R_{sl}	Schottky layer resistance
R_{gb}	Grain boundary resistance
R_g	Grain resistance
C_{el}	Electrode capacitance
C_{sl}	Schottky layer capacitance
C_{gb}	Grain boundary capacitance
C_g	Grain capacitance
C_∞	High-frequency limit of capacitance
L_S	Series stray inductance
Q_{CPE}	Pre-factor of CPE
Z_{CPE}	Impedance of CPE
m	Dispersion index of CPE
σ_{ac}	Alternating current conductivity

σ_{dc}	Direct current conductivity
$E_{a(gg)}$	Activation energy for grain growth
$E_{a(g)}$	Activation energy for grain
$E_{a(gb)}$	Activation energy for grain boundary
$E_{a(el)}$	Activation energy for electrode-interface
$E_{a(\sigma_{dc})}$	Activation energy for direct current conductivity
$E_{a(\sigma_{ac})}$	Activation energy for alternating current conductivity
$E_{a(\rho_{dc})}$	Activation energy for direct current specific resistivity
k_B	Boltzmann constant or constant of proportionality
A_D	Dispersive amplitude of Debye response
τ_D	Relaxation time of Debye response
A_{CC}	Dispersive amplitude of CC response
τ_{CC}	Relaxation time of CC response
α_{CC}	CC-associated empirical exponent
A_{CD}	Dispersive amplitude of CD response
τ_{CD}	Relaxation time of CD response
β_{CD}	CD-associated empirical exponent
A_{HN}	Dispersive amplitude of HN response
τ_{HN}	Relaxation time of HN response
α_{HN}, β_{HN}	HN-associated empirical exponents
$V_O^{\cdot\cdot}$	Doubly ionized oxygen vacancies
$h^{\cdot}$	Electronic holes
e'	Excess electrons
R^2	Correlation coefficient of linear fit
$\|Z\|$	Absolute impedance
θ_Z	Impedance phase
R_{wp}	Rietveld conceived of weighted profile R-factor
R_{exp}	Rietveld conceived of expected R-factor
R_p	Rietveld conceived of profile R-factor
χ^2	Goodness of fit value, $(R_{wp}/R_{exp})^2$

CHAPTER 1

INTRODUCTION

1.1 Research Background

Dielectrics, their breadth of discipline in general classified into physics, electrical engineering, materials science, and chemistry, are publicly recognized for their passive electrical insulation properties under the influence of magnetic, electric, or electromagnetic field. From a global perspective view yearly, the research output in the dielectric field is in the rapid ascending order, notably in South-East Asia countries which published considerable dielectric studies. As traced back to the early year before 1980, lead and barium-containing perovskite compounds have been the dominant scientific studies in various matter forms (polymer, ceramic, thin film, glass, rubber, liquid, gas) and were being investigated in the dielectric functions of polarization, relaxation, conduction, and high frequency phenomena. As time ages by, approaches have been taken toward driving down the extensive use of lead following its lifetime adverse effects on environment and human health. In particular, this cumulative metal toxicant poses a high exposure risk to the occupational health during the manufacture of lead zirconium titanate (PZT)-based nanotechnologies. Yet the demands of PZT-based high performance nanofabrication in sensors and actuators are dramatically growing since the discovery of pioneering PZT ceramic with exceptional piezoelectric properties by the Japanese physicists in 1952 (Shirane and Suzuki, 1952). In order to comply with the Restriction of Hazardous Substances Directive, lead-free and environment-friendly alternatives are of priority since year 2003 thereof, being the primary on-going quests for at least comparable piezoelectric and ferroelectric attributes to their lead counterparts. Until now, bismuth-based materials have gained the most popularity among the other non-toxic alternatives, being featured with superior properties across many disciplines as a consequence of their unique crystal structures. These types of lighter, synthetic materials are further described in the later section, whose foremost bismuth titanate ($Bi_4Ti_3O_{12}$) is meant to act as the parent subject for the present studied variants of related structures.

1.2 Understanding of Bismuth-based Aurivillius Ceramics

Bismuth (Bi)-based ceramics are undeniably categorized as one of the complex-oxide families of layered structural-type involving the basis of perovskite structure. The prototypical representation of layered Bi-containing oxides is $Bi_4Ti_3O_{12}$ (n = 3, being the number of oxygen octahedron that forms the pseudo-perovskite blocks), whose crystal structure as shown in Figure 1.2(a) is built by three interleaving pseudo-perovskite blocks $(Bi_2Ti_3O_{10})^{2-}$ between fluorite-like $(Bi_2O_2)^{2+}$ slabs stacked along a crystallographic c-direction. This sandwiched-like intergrowth configuration is known as Aurivillius phase, named in respect to Bengt Aurivillius who pioneered Bi_2O_3-TiO_2 solid solution in 1949 (Aurivillius, 1949). A general expression $(Bi_2O_2)^{2+}(A_{n-1}B_nO_{3n+1})^{2-}$ applicable to the exploiting of other homologous Aurivillius series in one crystallographic direction was developed. Here, the notations A and B are the cationic sites occupied by larger (i.e., mono, di, or

chemistry of Aurivillius phase to $A'[A_{n-1}B_nO_{3n+1}]$ of Dion-Jacobson phase (see Figure 1.4).

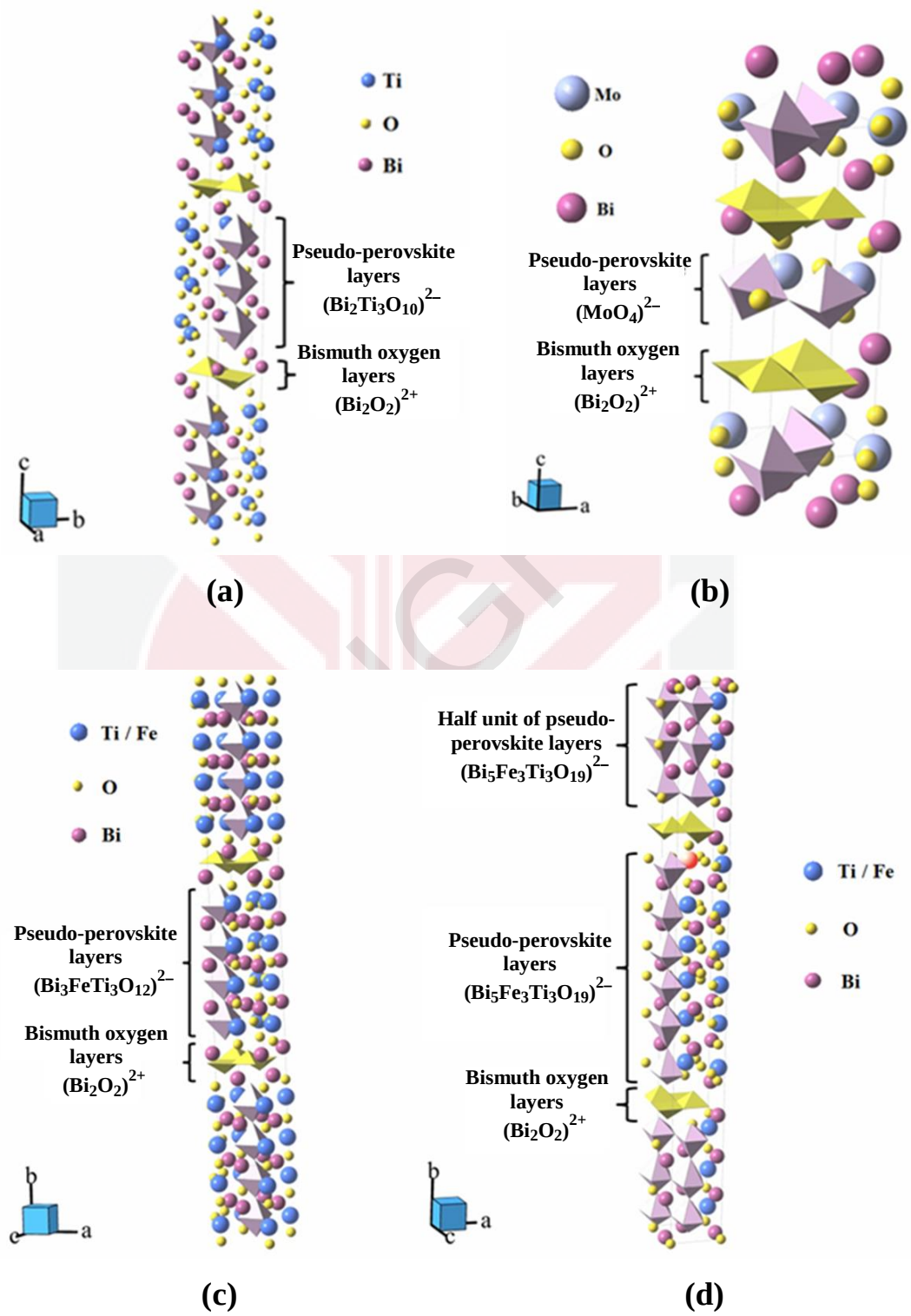

Figure 1.2: Aristotype Tetragonal Crystal Structure of Aurivillius Phase (a) n = 3 $Bi_4Ti_3O_{12}$, along with Other Orthorhombic-type Aurivillius Phases Characterized by Different Thicknesses of Perovskite-like Slabs as in (b) n = 1 Bi_2MoO_6, (c) n = 4 $Bi_5FeTi_3O_{15}$, and (d) n = 6 $Bi_7Fe_3Ti_3O_{21}$

of a high non-linear dielectric response. The phase transition of $Bi_4Ti_3O_{12}$ from tetragonal to orthorhombic structure (i.e. changes in the lattice parameters by lowering of symmetry as shown in Figure 1.8) upon cooling undergoes three structural distortions simultaneously as follows (Benedek et al., 2015):

a) Off-centering of Bi cation and O anion in the perovskite blocks.
b) Octahedral tilting along the crystallographic a-direction.
c) Rotation of oxygen octahedra around the crystallographic c-direction.

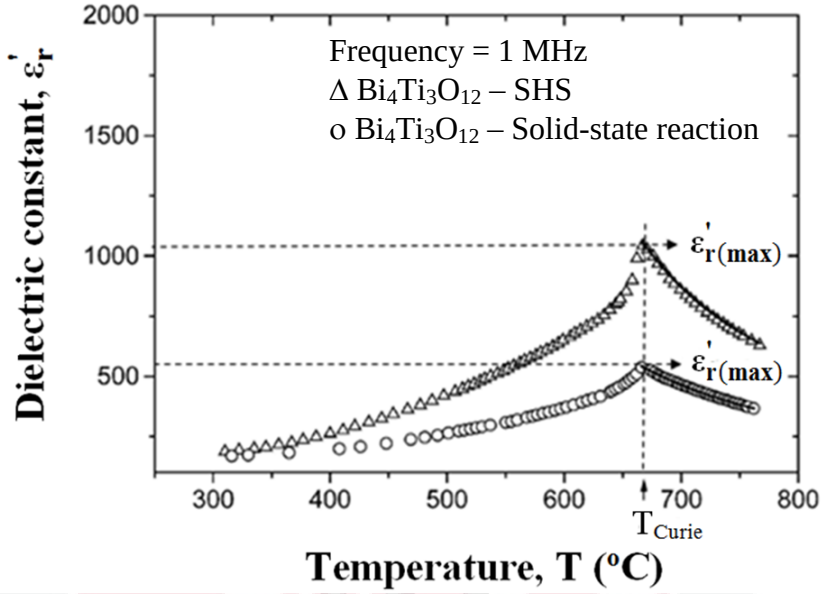

Figure 1.7: Curie Temperature T_{Curie} Determinations of $Bi_4Ti_3O_{12}$ at Constant Frequency 1 MHz. Note that the Samples were Produced via Self-propagating High-temperature Synthesis (SHS) and Solid State Reaction
(Source: Macedo et al., 2004)

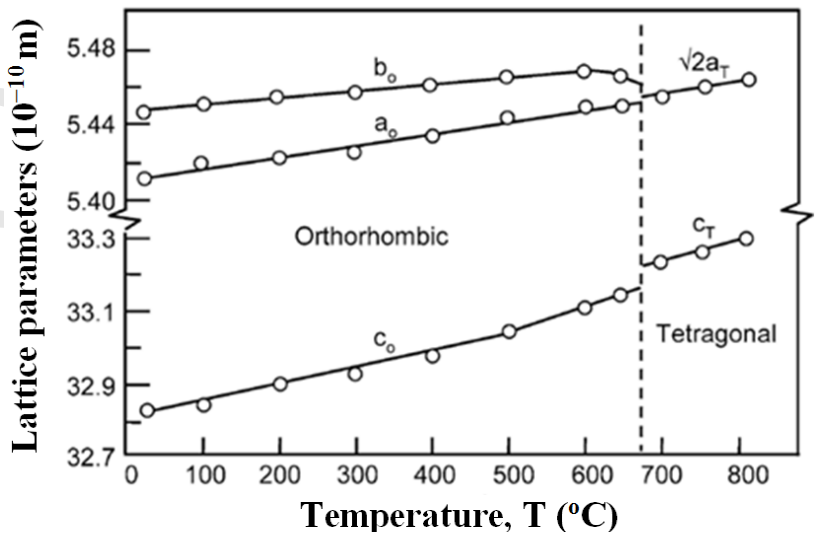

Figure 1.8: Phase Transition of $Bi_4Ti_3O_{12}$ with the Variation of Lattice Parameters as a Function of Temperature. Orthorhombic-associated Lattice Parameters are Indicated by a_o, b_o, and c_o; while Tetragonal-associated Lattice Parameters are Indicated by a_T and c_T, Respectively
(Source: Jardiel et al., 2008)

1.3 Problem Statement

Researches on Bi-layered oxides have always been accompanied by a number of shortcomings that tend to limit the leveraging of their key resources, varying according to the fabrication techniques. The expected challenges hereafter consider the solid state synthesis via conventional and high energy milling, both of which are employed in the current research. In the conventional processing, the reaction path takes place in two-steps heat treatment, opening up the possibility of causing the evaporation of bismuth oxide Bi_2O_3 species at high sintering temperatures due to its hygroscopic nature in Bi volatility. This is the unfavourable situation triggering conceivably the materials of non-stoichiometric form, thus leading to the consequences of having oxygen deficiencies and instability in oxidation state of titanium (Ti) ions in which the positioning and generation are difficult to control (Zhang et al., 2014; Siriprapa et al., 2013). The volatile species provokes further complication on the possible formation of intermediate phases upon sintering process, such as sillenite phase which reacts with the presence of precursor TiO_2 phase toward the synthesis of primary $Bi_4Ti_3O_{12}$ pure phase. Such temperature-driven transient intermediate phase formation may result in poor densification of the materials associated with exaggerated grain growth, dampening the dielectric properties which immediately raise a question on whether the usage of starting nanopowders herein would manage to provide improved reactivity for the densification of end product during the conventional sintering process.

The above mentioned inefficiencies in the conventional processing are practically preventable through the process of high energy milling. Such milling speed is apparently intense, being advantageous in avoiding the evaporation of Bi_2O_3 during the subsequent sintering as the volatile Bi ions are effectively relieved at the sites of high-impact ball collision where the mechanochemical reaction takes place in the condition of instant "hot spots" of localized heat and pressure (Friščić et al., 2013). As a result, mechanical energy is transferred into the system, providing mass transfer to achieve a potential direct milling synthesis of single-phase Bi-based material whilst inducing better sinterability for the concomitant formation of amorphous and crystalline phases. In some particular cases such as the pure and erbium (Er)-doped $Bi_5CrTi_3O_{15}$, the direct synthesis difficulties by intensive milling alone can be anticipated from the viewpoint of multi-valence configuration of chromium (Cr) cation and the strength of Er-cation substitution, thus the corresponding complete phase formations require sintering. Also these present a major concern in which the process ahead may stand a chance to leave behind a powder contamination to the end product. One of the many sources of contamination can be intuitively attributed to the adsorption of oxygen and nitrogen on the powder and mill media surfaces especially under the ambient atmosphere (Suryanarayana, 2004b), creating impurity problems that definitely constrain the study to some extent.

On dielectric data analysis, the interpretations of the variation of real and imaginary components of the complex permittivity have been a challenging goal in both theoretical and practical significances, especially under frequency domain response. The experimental dielectric data upon simulation require theoretical support to extract more detailed information about the polarization phenomena. On this matter,

an analytical dielectric function based on any superposition of the Debye, Cole-Cole, Cole-Davison, and Havriliak-Negami dispersion mechanisms plus a direct current conductivity term is taken into consideration (Grosse, 2014), which is useful to approximate the dispersion behaviour. As this fitting process is totally based on trial and error approach, figuring out the appropriate initial guess values for each parameter with sufficient accuracy becomes time consuming, being particularly challenging in Bi-based materials due to the anisotropy of properties on dielectric relaxation.

The origin of dielectric properties associated with these materials is always related to the oxygen vacancies, which raise a question of the ways the defects, or more specifically the missing oxygen atoms do the trick and to what degree they contribute to ion transport at the stage of different sintering temperatures in different processing methods. The challenge continues as to answer on how the emergence of rare-earth Er element as A-site substitute in influencing the dielectric properties of three-layered $Bi_4Ti_3O_{12}$ and four-layered $Bi_5CrTi_3O_{15}$ compounds, also, to what extent these modified materials might function when subjected to different sintering temperatures and processing methods. Since the best fits of each dielectric data follow algorithm that indeed is purely mathematical derived, it turns out to be an arduous task to shed light on the underlying physical nature governing the relaxation polarization. Therefore, other empirical dielectric functions such as the representations in terms of dielectric modulus, conductivity, and impedance are proposed, which are expected to convey the supportive physical processes from their perspectives.

1.4 Scope of Research

In this research, solid state reaction via conventional and high energy milling methods are employed to synthesize n = 3 $Bi_4Ti_3O_{12}$ and higher homologous Aurivillius oxides n = 4 $Bi_5CrTi_3O_{15}$ at various sintering temperatures ranging from 700°C to 1000°C. Following the same procedures, the base $Bi_4Ti_3O_{12}$ and $Bi_5CrTi_3O_{15}$ compounds are tuned by substituting single isovalent Er^{3+} cation composition on the Bi-sites of the structure, forming the modified $Bi_{3.25}Er_{0.75}Ti_3O_{12}$ compound and turning out to be the first time in synthesizing $Bi_{4.25}Er_{0.75}CrTi_3O_{15}$ compound. These series altogether are systematically made in attempting to answer the following utmost objectives:

1) To identify the role of Bi-site substitutional Er^{3+} cation and to make a comparison of methods between similar samples in view of the phase formation, microstructure, and dielectric properties.
2) To determine the underlying physical interpretations of the dielectric properties in the samples through an empirical fit of relaxation functions in the frequency range of 100 Hz – 10 MHz at room temperature and elevated temperatures in the range of 100 – 300°C.
3) To study the effect of sintering temperature on densification and microstructure that controls the dielectric properties of the samples.

1.5 Dissertation Organization

The dissertation is organized into five chapters. Up to this point we have built a better understanding of how the Bi-related Aurivillius ceramics behave and perform mostly in terms of crystallographic aspect. This is followed by the consideration of potential issues behind the synthesis and characterization. In addition, the present research directions and strategies are also clearly defined.

We continue in Chapter 2 with a specific review of the literatures concerning the synthesis of $Bi_4Ti_3O_{12}$ and its higher homologous derivatives, starting with the attempt to gather relevant scientific information limited to the published literatures on the solid state syntheses using conventional and high energy milling approaches. Following this manner, the subsequent discussion in the aspects of electrical and structural studies is developed, focusing on a wide range of past achievements relating to the parent and their modified Aurivillius compounds. The last discussion in this chapter is devoted to the practical significance of frequency domain in interpreting particularly the dielectric phenomena, and at this stage, to enter into the dielectric concept at the most fundamental level, as well as an outline of some aspects of presentation of dielectric data.

Chapter 3 provides a descriptive procedure of the synthesis techniques employed, detailing every process involved which begins with the sample preparation and ends with the methods of characterization and measurement. Chapter 4 presents a wide range of experimental findings. We begin with the interpretations of each system from thermal, crystallographic, and morphological analyses, all of which are made clearer independently according to the type of processing methods concerned. While presenting the room-temperature measured dielectric data involving the manipulated variable of frequency, the treatment of interpretational analysis based on an empirical fitting function is provided. In the same way, some significances of frequency domain dielectric response measured over a range of temperatures are highlighted. In order to make the fullest possible understanding of the frequency range of room-temperature measured dielectric data, impedance representations of these data are presented along with an equivalent circuit modelling. A comparison of processing methods evaluated from the aspect of dielectric analysis is also given. Chapter 5 concludes the main findings and suggests the prospect of future work.

BIBLIOGRAPHY

Aakansha, Deka, B., Ravi, S. and Pamu, D. (2017). Impedance spectroscopy and ac conductivity mechanism in Sm doped yttrium iron garnet. *Ceramics International*, 43(13), 10468-10477.

Afify, H. H., El Zawawi, I. K. and Battisha, I. K. (1999). Photoelectronic properties of (Cu, Fe, Al) incorporated CdS thin films. *Journal of Materials Science: Materials in Electronics*, 10(7), 497-502.

Impedance measurement handbook, a guide to measurement technology and techniques, 6th edition - Application note. (2016). Retrieved 13 October 2016 from http://literature.cdn.keysight.com/litweb/pdf/5950-3000.pdf

Algueró, M., Ferrer, P., Vila, E., Iglesias, J. E. and Castro, A. (2006). $Bi_4Ti_3O_{12}$ ceramics from powders prepared by alternative routes: Wet no-coprecipitation chemistry and mechanochemical activation. *Journal of the American Ceramic Society*, 89(11), 3340-3347.

Algueró, M., Gregg, J. M. and Mitoseriu, L. (2016). *Nanoscale Ferroelectrics and Multiferroics: Key Processing and Characterization Issues, and Nanoscale Effects*. New York: Wiley.

Aurivillius, B. (1949). Mixed bismuth oxides with layer lattices. II. Structure of $Bi_4Ti_3O_{12}$. *Arkiv for Kemi*, 1(54), 463-480.

Azlan, U. A. A., Krengvirat, W., Noor, A .F. M., Razak, K. A. and Sreekantan, S. (2012). Sintering and Characterization of Rare Earth Doped Bismuth Titanate Ceramics Prepared by Soft Combustion Synthesis. In A. Lakshmanan (Ed.), *Sintering of Ceramics - New Emerging Techniques* (pp. 357-378). Rijeka: InTech.

Bai, W., Chen, C., Yang, J., Zhang, Y., Qi, R., Huang, R., Tang, X., Duan, C. G. and Chu, J. (2015). Dielectric behaviors of Aurivillius $Bi_5Ti_3Fe_{0.5}Cr_{0.5}O_{15}$ multiferroic polycrystals: Determining the intrinsic magnetoelectric responses by impedance spectroscopy. *Scientific Reports*, 5, 17846.

Balaz, P. (2008). High-energy Milling. In *Mechanochemistry in Nanoscience and Minerals Engineering* (pp. 103-132). Berlin: Springer-Verlag Berlin Heidelberg.

Benedek, N. A., Rondinelli, J. M., Djani, H., Ghosez, P. and Lightfoot, P. (2015). Understanding ferroelectricity in layered perovskites: New ideas and insights from theory and experiments. *Dalton Transactions*, 44(23), 10543-10558.

Bernard, H., Lisińska-Czekaj, A., Dzik, J., Osińska, K. and Czekaj, D. (2011). Fabrication, structural and ac impedance studies of layer-structured $Bi_4Ti_3O_{12}$ ceramics. *Archives of Metallurgy and Materials*, 56(4), 1137-1148.

Bobić, J. D., Katiliute, R. M., Ivanov, M., Petrović, M. M. V., Ilić, N. I., Džunuzović, A. S., Banys, J. and Stojanović, B. D. (2016). Dielectric, ferroelectric and magnetic properties of La doped $Bi_5Ti_3FeO_{15}$ ceramics. *Journal of Materials Science: Materials in Electronics*, 27(3), 2448-2454.

Bobić, J. D., Petrović, M. M. V., Ilić, N. I., Palaimiene, E., Grigalaitis, R., Santos, C. O. P., Cilence, M. and Stojanović, B. D. (2015). Lead-free $BaBi_4Ti_4O_{15}$ ceramics: Effect of synthesis methods on phase formation and electrical properties. *Ceramics International*, 41(1), 309-316.

Bobić, J. D., Petrović, M. M. V. and Stojanović, B. D. (2013). Aurivillius $BaBi_4Ti_4O_{15}$ based compounds: Structure, synthesis and properties. *Processing and Application of Ceramics*, 7(3), 97-110.

Bokolia, R., Thakur, O. P., Rai, V. K., Sharma, S. K. and Sreenivas, K. (2015). Dielectric, ferroelectric and photoluminescence properties of Er^{3+} doped $Bi_4Ti_3O_{12}$ ferroelectric ceramics. *Ceramics International*, 41(4), 6055-6066.

Borse, P. H., Yoon, S. S., Jang, J. S., Lee, J. S., Hong, T. E., Jeong, E. D., Won, M. S., Jung, O. K., Shim, Y. B. and Kim, H. G. (2009). Formation of layered $Bi_5Ti_3FeO_{15}$ perovskite in Bi_2O_3-TiO_2-Fe_2O_3 containing system. *Bulletin of the Korean Chemical Society*, 30(12), 3011-3015.

Bugnet, M., Kula, A., Niewczas, M. and Botton, G. A. (2014). Segregation and clustering of solutes at grain boundaries in Mg-rare earth solid solutions. *Acta Materialia*, 79, 66-73.

Chang, H. H., Cheng, C. L., Huang, P. J. and Lin, S. Y. (2014). Application of scanning electron microscopy and X-ray microanalysis: FE-SEM, ESEM-EDS, and EDS mapping for studying the characteristics of topographical microstructure and elemental mapping of human cardiac calcified deposition. *Analytical and Bioanalytical Chemistry*, 406(1), 359-366.

Chen, H. B., Shen, B., Xu, J. B. and Zhai, J. W. (2013). The grain size-dependent electrical properties of $Bi_4Ti_3O_{12}$ piezoelectric ceramics. *Journal of Alloys and Compounds*, 551, 92-97.

Chen, J., Luo, L., Lin, J. S., Zan, X., Zhu, X., Luo, G. and Wu, Y. (2017). Influence of ball milling processing on the microstructure and characteristic of W–Nb alloy. *Journal of Alloys and Compounds*, 694, 905-913.

Chokshi, A. H. (2008). Triple junction limited grain growth in nanomaterials. *Scripta Materialia*, 59(7), 726-729.

Cveticanin, L. (2014). On the truly nonlinear oscillator with positive and negative damping. *Applied Mathematics and Computation*, 243, 433-445.

Da Silva, K. L., Menzel, D., Feldhoff, A., Kübel, C., Bruns, M., Paesano, A., Düvel, A., Wilkening, M., Ghafari, M., Hahn, H., Litterst, F. J., Heitjans, P., Becker, K. D. and Šepelák, V. (2011). Mechanosynthesized $BiFeO_3$ nanoparticles with highly reactive surface and enhanced magnetization. *The Journal of Physical Chemistry C*, 115(15), 7209-7217.

Dercz, J., Dercz, G., Prusik, K., Hanc, A., Babilas, R., Pajak, L. and Milczuk, J. (2009a). Structure investigation of $Bi_5Ti_3FeO_{15}$ ceramics prepared by free sintering process of high-energy ball milled nanocrystalline precursors. *Archives of Metallurgy and Materials*, 54(3), 741-746.

Dercz, J., Dercz, G., Prusik, K., Solecka, B., Starczewska, A. and Ilczuk, J. (2009b). Influence of primary milling on structural and electrical properties of $Bi_4Ti_3O_{12}$ ceramics obtained by sintering process. *International Journal of Thermophysics*, 31(1), 42-54.

Dercz, J., Starczewska, A. and Dercz, G. (2011). Dielectric and structural properties of $Bi_5Ti_3FeO_{15}$ ceramics obtained by solid-state reaction process from mechanically activated precursors. *International Journal of Thermophysics*, 32(4), 746-761.

Dillon, S. J., Behera, S. K. and Harmer, M. P. (2008). An experimentally quantifiable solute drag factor. *Acta Materialia*, 56(6), 1374-1379.

Drdlíková, K., Klement, R., Drdlík, D., Spusta, T., Galusek, D. and Maca, K. (2017). Luminescent Er^{3+} doped transparent alumina ceramics. *Journal of the European Ceramic Society*, 37(7), 2695-2703.

Dyre, J. C. and Schroeder, T. B. (2004). Hopping models for ion conduction in noncrystals. *Physics*, 97-102.

Elissalde, C. and Ravez, J. (2001). Ferroelectric ceramics: Defects and dielectric relaxations. *Journal of Materials Chemistry*, 11(8), 1957-1967.

Elliott, S. R. (1989). A model for non-Debye relaxation in ionically conducting glasses. *Materials Science and Engineering B*, 3(1-2), 69-72.

Fang, Z. Z., Wang, H. and Kumar, V. (2017). Coarsening, densification, and grain growth during sintering of nano-sized powders - A perspective. *International Journal of Refractory Metals and Hard Materials*, 62, 110-117.

Faure, B., Salazar-Alvarez, G., Ahniyaz, A., Villaluenga, I., Berriozabal, G., De Miguel, Y. R. and Bergström, L. (2013). Dispersion and surface functionalization of oxide nanoparticles for transparent photocatalytic and UV-protecting coatings and sunscreens. *Science and Technology of Advanced Materials*, 14(2), 23001.

Fewster, P. F. (2014). A new theory for X-ray diffraction. *Acta Crystallographica Section A: Foundations and Advances*, 70(3), 257-282.

Friščić, T., Halasz, I., Beldon, P. J., Belenguer, A. M., Adams, F., Kimber, S. A. J., Honkimäki, V. and Dinnebier, R. E. (2013). Real-time and in situ monitoring of mechanochemical milling reactions. *Nature Chemistry*, 5(1), 66-73.

Geng, H., Ji, Y., Feng, X., Zhang, J., Gao, Y., Yan, Y., Wang, W. Q., Su, F. and Du, X. (2016). Preparing $Sm_2Fe_{17}C_x$ compound by high-energy ball-milling Sm-Fe alloy in heptane followed by annealing, re-milling and re-annealing. *Materials & Design*, 111, 140-145.

Giddings, A. T., Stennett, M. C., Reid, D. P., McCabe, E. E., Greaves, C. and Hyatt, N. C. (2011). Synthesis, structure and characterisation of the n=4 Aurivillius phase $Bi_5Ti_3CrO_{15}$. *Journal of Solid State Chemistry*, 184(2), 252-263.

Gil Novoa, O. D., Landínez Téllez, D. A. and Roa-Rojas, J. (2012). Synthesis and structural and electrical characterization of new materials $Bi_3R_2FeTi_3O_{15}$. *Physica B: Condensed Matter*, 407(16), 3099-3101.

Golda, R. A., Marikani, A. and Padiyan, D. P. (2011). Mechanical synthesis and characterization of $Bi_4Ti_3O_{12}$ nanopowders. *Ceramics International*, 37(8), 3731-3735.

Gong, M. M., Dey, S., Wu, L. J., Chang, C. H., Li, H., Castro, R. H. R. and Liu, F. (2017). Effects of concurrent grain boundary and surface segregation on the final stage of sintering: the case of lanthanum doped yttria-stabilized zirconia. *Journal of Materials Science and Technology*, 33(3), 251-260.

Gottstein, G., Ma, Y. and Shvindlerman, L. S. (2005). Triple junction motion and grain microstructure evolution. *Acta Materialia*, 53(5), 1535-1544.

Greenleaf, M. (2014). *Phenomenological Equivalent Circuit Modeling of Various Energy Storage Devices*. (PhD Thesis). Florida State University, USA.

Grosse, C. (2014). A program for the fitting of Debye, Cole-Cole, Cole-Davidson, and Havriliak-Negami dispersions to dielectric data. *Journal of Colloid and Interface Science*, 419, 102-106.

Han, K. S. and Ko, T. Y. (2009). Synthesis and phase formation of ferroelectric $Bi_4Ti_3O_{12}$ nanopowder by mechanical alloying. *Journal of Alloys and Compounds*, 473(1-2), 490-495.

Henderson, T. M., Greer, J. C., Bersuker, G., Korkin, A. and Bartlett, R. J. (2006). Effect of Chemical Environment and Strain on Oxygen Vacancy Formation Energies at Silicon-silicon Oxide Interfaces. In E. Gusev (Ed.), *Defects in High-k Gate Dielectric Stacks* (pp. 373-383). Dordrecht: Springer Netherlands.

Holm, E. A., Miodownik, M. A. and Rollett, A. D. (2003). On abnormal subgrain growth and the origin of recrystallization nuclei. *Acta Materialia*, 51(9), 2701-2716.

Hu, J. and Shen, Z. (2012). Grain growth by multiple ordered coalescence of nanocrystals during spark plasma sintering of $SrTiO_3$ nanopowders. *Acta Materialia*, 60(18), 6405-6412.

Hu, S. Y., Li, Y. L., Zheng, Y. X. and Chen, L. Q. (2004). Effect of solutes on dislocation motion - A phase-field simulation. *International Journal of Plasticity*, 20(3), 403-425.

Hu, W., Liu, Y., Withers, R. L., Frankcombe, T. J., Norén, L., Snashall, A., Kitchin, M., Smith, P., Gong, B., Chen, H., Schiemer, J., Brink, F. and Leung, W. J. (2013). Electron-pinned defect-dipoles for high-performance colossal permittivity materials. *Nature Materials*, 12(9), 821-826.

Humphreys, F. J. and Hatherly, M. (2004). Recrystallization of Single-phase Alloys. In *Recrystallization and Related Annealing Phenomena* (pp. 215-267). Amsterdam: Elsevier.

Jardiel, T., Caballero, A. C. and Villegas, M. (2008). Aurivillius ceramics: $Bi_4Ti_3O_{12}$-based piezoelectrics. *Journal of the Ceramic Society of Japan*, 116(4), 511-518.

Jeong, S., Na, H., Lee, G., Son, S. H. and Choi, H. (2014). Cross-sectional analysis of W-cored Ni nanoparticle via focused ion beam milling with impregnation. *Nanoscale Research Letters*, 9(1), 533.

Jiang, C., Zhou, K., Zhou, X., Li, Z. and Zhang, D. (2015). Synthesis and characterization of $Na_{0.5}Bi_{0.5}TiO_3$ platelets with preferred orientation using Aurivillius precursors. *Ceramics International*, 41(5), 6858-6862.

Jonscher, A. K. (1978). Analysis of the alternating current properties of ionic conductors. *Journal of Materials Science*, 13(3), 553-562.

Jonscher, A. K. (1983a). Previously Accepted Interpretations. In *Dielectric Relaxation in Solids* (pp. 294-309). London: Chelsea Dielectrics Press.

Jonscher, A. K. (1983b). The Dynamic Response of Idealised Physical Models. In *Dielectric Relaxation in Solids* (pp. 116-158). London: Chelsea Dielectric Press.

Jonscher, A. K. (1995). An electrochemical model of low-frequency dispersion. *Journal of Materials Science*, 30(10), 2491-2495.

Jonscher, A. K. (1996). Measurement and Presentation of Data. In *Universal Relaxation Law* (pp. 263-307). London: Chelsea Dielectric Press.

Jonscher, A. K. and Deori, K. L. (1979). The dielectric response of $K_xAl_xTi_{8-x}O_{16}$ and $K_xMg_{x/2}Ti_{8-x/2}O_{16}$. *Journal of Materials Science*, 14, 1308-1320.

Kelly, M. N., Bojarski, S. A. and Rohrer, G. S. (2017). The temperature dependence of the relative grain-boundary energy of yttria-doped alumina. *Journal of the American Ceramic Society*, 100(2), 783-791.

Kikkawa, S., Sun, S., Masubuchi, Y., Nagamine, Y. and Shibahara, T. (2016). Ferroelectric response induced in cis-type anion ordered $SrTaO_2N$ oxynitride perovskite. *Chemistry of Materials*, 28(5), 1312-1317.

Kim, H. S., Madavali, B., Eom, T. J., Kim, C. M., Koo, J. M., Lee, T. H. and Hong, S. J. (2015). Effect of different mechanical milling processes on morphology and microstructural changes of nano and micron Al-powders. *Archives of Metallurgy and Materials*, 60(2), 1235-1239.

Kimura, T., Yi, Y. and Sakurai, F. (2010). Mechanisms of texture development in lead-free piezoelectric ceramics with perovskite structure made by the templated grain growth process. *Materials*, 3(11), 4965-4978.

Klimkowicz, A., Świerczek, K., Yamazaki, T. and Takasaki, A. (2016). Enhancement of the oxygen storage properties of $BaPrMn_2O_{5+\delta}$ and $BaSmMn_2O_{5+\delta}$ oxides by a high-energy milling. *Solid State Ionics*, 298, 66-72.

Knyazev, A. V., Krasheninnikova, O. V., Smirnova, N. N., Shushunov, A. N., Syrov, E. V. and Blokhina, A. G. (2015). Thermodynamic properties and X-ray diffraction of $Bi_4Ti_3O_{12}$. *Journal of Thermal Analysis and Calorimetry*, 122(2), 747-754.

Kong, L. B., Ma, J., Zhu, W. and Tan, O. K. (2001). Preparation of $Bi_4Ti_3O_{12}$ ceramics via a high-energy ball milling process. *Materials Letters*, 51(2), 108-114.

Kuang, X., Bridges, C., Allix, M., Claridge, J. B., Hughes, H. and Rosseinsky, M. J. (2006). Internal barrier layer capacitance effect in hexagonal perovskite $Ba_4YMn_3O_{11.5}$ ceramics. *Chemistry of Materials*, 18(21), 5130-5136.

Lallemant, L., Roussel, N., Fantozzi, G., Garnier, V., Bonnefont, G., Douillard, T., Durand, B., Guillemet-Fritsch, S., Chane-Ching, J. Y., Garcia-Gutierez, D. and Aguilar-Garib, J. (2014). Effect of amount of doping agent on sintering, microstructure and optical properties of Zr- and La-doped alumina sintered by SPS. *Journal of the European Ceramic Society*, 34(5), 1279-1288.

Lehtimäki, M. (2013). *Stability, Cation Ordering and Oxygen Non-stoichiometry of Some Perovskites and Related Layered Oxides*. (PhD Thesis). Aalto University, Finland.

Liu, C., Liu, X., Tan, J., Wang, Q., Wen, H. and Zhang, C. (2017). Nitrogen-doped graphene by all-solid-state ball-milling graphite with urea as a high-power lithium ion battery anode. *Journal of Power Sources*, 342, 157-164.

Liu, W., Wang, Q., Zhang, J., Xie, X., Liu, H., Min, G. and Xia, B. (2016). Isothermal kinetic analysis of the effects of high-energy ball milling on solid-state reaction of $Li_4Ti_5O_{12}$. *Powder Technology*, 287, 373-379.

Lomanova, N. A., Morozov, M. I., Ugolkov, V. L. and Gusarov, V. V. (2006). Properties of Aurivillius phases in the $Bi_4Ti_3O_{12}$-$BiFeO_3$ system. *Inorganic Materials*, 42(2), 189-195.

Lomanova, N. A., Semenov, V. G., Panchuk, V. V. and Gusarov, V. V. (2012). Structural changes in the homologous series of the Aurivillius phases $Bi_{n+1}Fe_{n-3}Ti_3O_{3n+3}$. *Journal of Alloys and Compounds*, 528, 103-108.

Long, C. B., Chang, Q. and Fan, H. Q. (2017). Differences in nature of electrical conductions among $Bi_4Ti_3O_{12}$-based ferroelectric polycrystalline ceramics. *Scientific Reports*, 7, 4193.

Lukichev, A. A. (2014). Relaxation function for the non-Debye relaxation spectra description. *Chemical Physics*, 428, 29-33.

Macdonald, J. R. (1992). Impedance spectroscopy. *Annals of Biomedical Engineering*, 20(3), 289-305.

Macedo, Z. S., Ferrari, C. R. and Hernandes, A. C. (2004). Impedance spectroscopy of $Bi_4Ti_3O_{12}$ ceramic produced by self-propagating high-temperature synthesis technique. *Journal of the European Ceramic Society*, 24(9), 2567-2574.

Mandal, P. R. and Nath, T. K. (2015). Oxygen-vacancy and charge hopping related dielectric relaxation and conduction process in orthorhombic Gd doped $YFe_{0.6}Mn_{0.4}O_3$ multiferroics. *Journal of Alloys and Compounds*, 628, 379-389.

Marsh, C., Depinoy, S. and Kaoumi, D. (2016). Effect of heat treatment on the temperature dependence of the fracture behavior of X-750 alloy. *Materials Science and Engineering A*, 677, 474-484.

Matsui, K. and Hojo, J. (2008). Sintering kinetics at constant rates of heating: Effect of GeO_2 addition on the initial sintering stage of 3 mol% Y_2O_3-doped zirconia powder. *Journal of Materials Science*, 43(3), 852-859.

Mießen, C., Liesenjohann, M., Barrales-Mora, L. A., Shvindlerman, L. S. and Gottstein, G. (2015). An advanced level set approach to grain growth - Accounting for grain boundary anisotropy and finite triple junction mobility. *Acta Materialia*, 99, 39-48.

Mohapatra, S. R., Sahu, B., Chandrasekhar, M., Kumar, P., Kaushik, S. D., Rath, S. and Singh, A. K. (2016). Effect of cobalt substitution on structural, impedance, ferroelectric and magnetic properties of multiferroic $Bi_2Fe_4O_9$ ceramics. *Ceramics International*, 42(10), 12352-12360.

Murali, N., Margarette, S. J., Kumar, G. P., Sailaja, B., Mulushoa, S. Y., Himakar, P., Babu, B. K. and Veeraiah, V. (2017). Effect of Al substitution on the structural and magnetic properties of Co-Zn ferrites. *Physica B: Condensed Matter*, 522, 1-6.

Navarro-Rojero, M. G., Romero, J. J., Rubio-Marcos, F. and Fernandez, J. F. (2010). Intermediate phases formation during the synthesis of $Bi_4Ti_3O_{12}$ by solid state reaction. *Ceramics International*, 36(4), 1319-1325.

Naveed-Ul-Haq, M., Shvartsman, V. V., Salamon, S., Wende, H., Trivedi, H., Mumtaz, A. and Lupascu, D. C. (2016). A new (Ba, Ca) (Ti, Zr)O_3 based multiferroic composite with large magnetoelectric effect. *Scientific Reports*, 6, 32164.

Ortuño, M., Somoza, A. M., Vinokur, V. M. and Baturina, T. I. (2015). Electronic transport in two-dimensional high dielectric constant nanosystems. *Scientific Reports*, 5, 9667.

Oz, A., Hershkovitz, S., Belman, N., Tal-Gutelmacher, E. and Tsur, Y. (2016). Analysis of impedance spectroscopy of aqueous supercapacitors by evolutionary programming: Finding DFRT from complex capacitance. *Solid State Ionics*, 288, 311-314.

Özdemir, Z. G., Kılıç, M., Karabul, Y., Mısırlıoğlu, B. S., Çataltepe, Ö. A. and İçelli, O. (2017). Synthesis and characterization of $EuBa_2Ca_2Cu_3O_{9-x}$: The influence of temperature on dielectric properties and charge transport mechanism. *Materials Science in Semiconductor Processing*, 63, 196-202.

Paul, J., Bhardwaj, S., Sharma, K. K., Kotnala, R. K. and Kumar, R. (2015). Room temperature multiferroic behaviour and magnetoelectric coupling in Sm/Fe modified $Bi_4Ti_3O_{12}$ ceramics synthesized by solid state reaction method. *Journal of Alloys and Compounds*, 634, 58-64.

Pedro-García, F., Sánchez-De, J. F., Cortés-Escobedo, C. A., Barba-Pingarrón, A. and Bolarín-Miró, A. M. (2017). Mechanically assisted synthesis of multiferroic $BiFeO_3$: Effect of synthesis parameters. *Journal of Alloys and Compounds*, 711, 77-84.

Peláez-Barranco, A., Guerra, J. D. S., López-Noda, R. and Araújo, E. B. (2008). Ionized oxygen vacancy-related electrical conductivity in $(Pb_{1-x}La_x)(Zr_{0.90}Ti_{0.10})_{1-x/4}O_3$ ceramics. *Journal of Physics D: Applied Physics*, 41(21), 215503.

Priyambada, N., Tanmaya, B., Anil, K. S. and Simanchalo, P. (2017). An approach for correlating the structural and electrical properties of Zr^{4+}-modified $SrBi_4Ti_4O_{15}$/SBT ceramic. *RSV Advances*, 7, 16319.

Prokip, V., Utkin, A., Baklanova, N., Cherkov, A., Zaitsev, B. and Mikheev, A. (2015). Synthesis of zirconium and hafnium germanates from mechanically activated oxides. *Ceramics International*, 41(6), 7963-7970.

Raabe, D., Herbig, M., Sandlöbes, S., Li, Y., Tytko, D., Kuzmina, M., Ponge, D. and Choi, P. P. (2014). Grain boundary segregation engineering in metallic alloys: A pathway to the design of interfaces. *Current Opinion in Solid State and Materials Science*, 18(4), 253-261.

Rachna, S., Bhattacharyya, S. and Gupta, S. M. (2010). Correlating structure, dielectric and impedance studies with lanthanum-ion substitution in bismuth titanate. *Materials Science and Engineering B*, 175(3), 207-212.

Rehman, F., Jin, H. B., Wang, L., Tanver, A., Su, D. Z. and Li, J. B. (2016). Effect of Nd^{3+} substitution for Bi^{3+} on the dielectric properties and conduction behavior of Aurivillius $NdBi_4Ti_3FeO_{15}$ ceramics. *RSC Advances*, 6(25), 21254-21260.

Reyes, P. and Velumani, S. (2012). Structural and optical characterization of mechanochemically synthesized copper doped CdS nanopowders. *Materials Science and Engineering B*, 177(16), 1452-1459.

Rios, P. R., Siciliano, J. F., Sandim, H. R. Z., Plaut, R. L. and Padilha, A. F. (2005). Nucleation and growth during recrystallization. *Materials Research*, 8(3), 225-238.

Riu, D. H., Kong, Y. M. and Kim, H. E. (2000). Effect of Cr_2O_3 addition on microstructural evolution and mechanical properties of Al_2O_3. *Journal of the European Ceramic Society*, 20(10), 1475-1481.

Rymarczyk, J., Machura, D. and Ilczuk, J. (2008). Processing and some properties of biferroic $Bi_5Ti_3FeO_{15}$ ceramics. *The European Physical Journal Special Topics*, 154(1), 187-190.

Shahzad, S. N. M., Qureshi, A. H., Waqas, H., Hussain, N., Saeed, K. and Ali, L. (2011). Investigation of phases developed in $Bi_4Ti_3O_{12}$ system by thermal and analytical techniques. *The Nucleus*, 48(2), 101-106.

Shibuta, Y., Oguchi, K., Takaki, T. and Ohno, M. (2015). Homogeneous nucleation and microstructure evolution in million-atom molecular dynamics simulation. *Scientific Reports*, 5, 13534.

Shirane, G. and Suzuki, K. (1952). Crystal structure of Pb(Zr, Ti)O_3. *Journal of the Physical Society of Japan*, 7(3), 333.

Shoar, A. M. R., Berkemeier, F., Schmitz, G. and Wilmer, D. (2009). On the physical interpretation of constant phase elements. *Solid State Ionics*, 180(14-16), 922-927.

Shpotyuk, O., Kozdras, A., Demchenko, P., Shpotyuk, Y., Bujňáková, Z. and Baláž, P. (2016). Solid-state amorphization of $As_{45}S_{55}$ alloy induced by high-energy mechanical milling. *Thermochimica Acta*, 642, 59-66.

Singh, R. S., Bhimasankaram, T., Kumar, G. S. and Suryanarayana, S. V. (1994). Dielectric and magnetoelectric properties of $Bi_5FeTi_3O_{15}$. *Solid State Communications*, 91(7), 567-569.

Siriprapa, P., Watcharapasorn, A. and Jiansirisomboon, S. (2013). Effects of Mn-dopant on phase, microstructure and electrical properties in $Bi_{3.25}La_{0.75}Ti_3O_{12}$ ceramics. *Ceramics International*, 39, S355-358.

Stallinga, P. (2011). Electronic transport in organic materials: Comparison of band theory with percolation/(variable range) hopping theory. *Advanced Materials*, 23(30), 3356-3362.

Steele, B., Burns, A. D., Chernatynskiy, A., Grimes, R. W. and Phillpot, S. R. (2010). Anisotropic thermal properties in orthorhombic perovskites. *Journal of Materials Science*, 45(1), 168-176.

Stojanović, B. D., Paiva-Santos, C. O., Cilense, M., Jovalekić, Č. and Lazarević, Z. Ž. (2008). Structure study of $Bi_4Ti_3O_{12}$ produced via mechanochemically assisted synthesis. *Materials Research Bulletin*, 43(7), 1743-1753.

Sui, J., Zheng, L., Zhang, X., Chen, Y. and Cheng, Z. (2016). A novel equivalent agglomeration model for heat conduction enhancement in nanofluids. *Scientific Reports*, 6, 19560.

Suryanarayana, C. (2004a). Introduction. In *Mechanical Alloying and Milling* (pp. 1-10). New York: CRC Press.

Suryanarayana, C. (2004b). Powder Contamination. In *Mechanical Alloying and Milling* (pp. 385-402). New York: CRC Press.

Suryanarayana, S. V. and Norton, M. G. (1998). Practical Aspects of X-ray Diffraction. In *X-Ray Diffraction: A Practical Approach* (pp. 63-93). New York: Plenum Press.

Tan, F. K., Hassan, J., Wahab, Z. A. and Azis, R. S. (2016). Electrical conductivity and dielectric studies of MnO_2 doped V_2O_5. *Results in Physics*, 6, 420-427.

Tang, R. J., Jiang, C., Qian, W. H., Jian, J., Zhang, X., Wang, H. Y. and Yang, H. (2015). Dielectric relaxation, resonance and scaling behaviors in $Sr_3Co_2Fe_{24}O_{41}$ hexaferrite. *Scientific Reports*, 5, 13645.

Thakur, P. Y., Ram, M. Y. and Dinesh, P. S. (2012). Mechanical milling: A top down approach for the synthesis of nanomaterials and nanocomposites. *Nanoscience and Nanotechnology*, 2(3), 22-48.

Thermogravimetry for routine and research. (2012). Retrieved 31 October 2016 from https://www.mt.com/dam/Analytical/ThermalAnalysi/TA-PDF/30064774_V10.12_TGA1_Brochure_en.pdf

Tselev, A., Brooks, C. M., Anlage, S. M., Zheng, H., Salamanca-Riba, L., Ramesh, R. and Subramanian, M. A. (2004). Evidence for power-law frequency dependence of intrinsic dielectric response in the $CaCu_3Ti_4O_{12}$. *Physical Review B*, 70(14), 144101.

Ullah, M., Ali, M. E. and Hamid, S. B. A. (2014). Surfactant-assisted ball milling: A novel route to novel materials with controlled nanostructure - A review. *Review of Advanced Materials Science*, 37, 1-14.

van de Graad, V. (2014). *Calculating the Reactive Power Using the Kramers-Kronig Relations*. (Bachelor's Thesis). Technische Universiteit Delft, Netherlands.

van Turnhout, J. (2016). Better resolved low frequency dispersions by the apt use of Kramers-Kronig relations, differential operators, and all-in-1 modeling. *Frontiers in Chemistry*, 4, 1-19.

Vlasenko, V. G., Shuvaeva, V. A., Levchenkov, S. I., Zubavichus, Y. V. and Zubkov, S. V. (2014). Structural, electrical and magnetic characterisation of a new Aurivillius phase $Bi_{5-x}Th_xFe_{1+x}Ti_{3-x}O_{15}$ (x = 1/3). *Journal of Alloys and Compounds*, 610: 184-188.

Wang, C. and Chen, S. H. (2012a). Factors influencing particle agglomeration during solid-state sintering. *Acta Mechanica Sinica*, 28(3), 711-719.

Wang, C. and Chen, S. H. (2012b). The effect of agglomerate on micro-structural evolution in solid-state sintering. *Acta Mechanica Sinica*, 28(5), 1323-1330.

Wang, J., Wang, Y., Liu, Y., Li, J., He, L. and Zhang, C. (2015). Densification and microstructural evolution of a high niobium containing TiAl alloy consolidated by spark plasma sintering. *Intermetallics*, 64, 70-77.

Watcharapasorn, A., Siriprapa, P. and Jiansirisomboon, S. (2010). Grain growth behavior in bismuth titanate-based ceramics. *Journal of the European Ceramic Society*, 30(1), 87-93.

Wei, T., Zhou, Q. J., Zhao, C. Z., Lin, Y. B., Zou, Y. L., Li, Y. and Zhang, L. S. (2013). Strong green light emission in Ho doped $Bi_4Ti_3O_{12}$ ferroelectric ceramics. *Ceramics International*, 39(6), 7211-7215.

Williams, G. and Thomas, D. K. (1998). Phenomenological and molecular theories of dielectric and electrical relaxation of materials. *Novocontrol Application Note Dielectrics*, 3, 1-29.

Wu, M. S., Tian, Z. M., Yuan, S. L., Duan, H. N. and Qiu, Y. (2012). Dielectric behavior and ac conductivity in Aurivillius $Bi_4Ti_3O_{12}$ doped by antiferromagnetic $BiFeO_3$. *Physics Letters A*, 376(28-29), 2062-2066.

Yang, F., Guo, Y. C., Li, L. Y. and Tang, M. H. (2016). Anisotropic polarization fatigue in $Bi_{3.15}Nd_{0.85}Ti_3O_{12}$ thin films. *Journal of Physics D: Applied Physics*, 49(19), 195305-195311.

Yang, H., Yan, F., Lin, Y., Wang, T. and Wang, F. (2017). High energy storage density over a broad temperature range in sodium bismuth titanate-based lead-free ceramics. *Scientific Reports*, 7, 8726.

Yin, W., Chen, C., Bai, W., Yang, J., Zhang, Y., Tang, X., Duan, C. G. and Chu, J. (2016). Dielectric behavior dependence on temperature and Cr-doping contents of Aurivillius $Bi_5Ti_3FeO_{15}$ ceramics. *Ceramics International*, 42(3), 4298-4305.

Zangina, T., Hassan, J., Matori, K. A., Azis, R. S., Ahmadu, U. and See, A. (2016). Sintering behavior, ac conductivity and dielectric relaxation of $Li_{1.3}Ti_{1.7}Al_{0.3}(PO_4)_3$ NASICON compound. *Results in Physics*, 6, 719-725.

Zhang, K. H. L., Sushko, P. V., Colby, R., Du, Y., Bowden, M. E. and Chambers, S. A. (2014). Reversible nano-structuring of $SrCrO_{3-\delta}$ through oxidation and reduction at low temperature. *Nature Communications*, 5, 4669.

Zhao, Y. H., Jin, Z. H. and Lu, K. (1999). Mechanical-milling-induced amorphization of Se: A crystallite destabilization model. *Philosophical Magazine Letters*, 79(9), 747-754.

Zheng, X. J., Peng, J. F., Chen, Y. Q., He, L., Feng, X., Zhang, D. Z., Gong, L. J. and Wu, Q. Y. (2010). Enhancement on effective piezoelectric coefficient of $Bi_{3.25}Eu_{0.75}Ti_3O_{12}$ ferroelectric thin films under moderate annealing temperature. *Thin Solid Films*, 519(2), 714-718.